

Research article

Numerical Simulation for Nutrients Propagation and Microbial Growth Using Finite Difference Approximation Technique

Prof. Dr. Vishwa Nath Maurya

Department of Mathematics, School of Science & Technology, University of Fiji, Saweni, Fiji
Formerly Director, Vision Institute of Technology, G.B. Technical University, India
E-mail: prof.drvmmaurya@gmail.com, prof_vnmaurya@yahoo.in

Abstract

Present paper demonstrates mathematical modelling and numerical simulation for microbial transport, nutrients propagation and microbial growth in the porous media. Particularly an attempt is made here for Microbial Enhance Oil Recovery (MEOR) which is a technology that involves the use of microorganisms to extract the remaining oil from the reservoir with an exceptionally low operating cost. The reservoir was assumed to be a perfect rectangular shape and was sub-divided into five grid blocks. The bacteria and nutrients were injected into the first grid block for the period of 10 days before the well was shut-in. After the shut-in, the concentration of bacteria and nutrient consumption rate were calculated in the other grid blocks with time. The simulated results explored in the present study have been compared with the plant data obtained from Garzan oil field. The simulated results obtained herein give us an idea about those bacteria concentration increased as the nutrients were consumed with time. However, during the fourth time step (40 days) of the soaking process, severe bacteria decay occurred due to the lack of sufficient nutrients.

Keywords: Mathematical modelling, Microbial Enhance Oil Recovery Technology, Microbe soaking period, Simulation, porous media

1. Introduction

Enhanced Oil Recovery (EOR) methods are used in the oil industry to increase the ultimate recovery of crude oil. This normally involves the application of an EOR method (sometimes called tertiary recovery method) to a specific underground oil bearing reservoir. Examples of well-known tertiary recovery methods are chemical flooding, miscible CO₂ injection and thermally enhanced oil recovery that uses heat as main source of additional recovery (Lake, 2005). Significant volumes of residual oil in the depleted oil reservoirs could be produced by these EOR methods as current technology leaves about two third of the original oil in place in the reservoir. One of such method is microbial enhanced oil recovery (MEOR). MEOR represents the use of microorganisms to extract the remaining oil from the reservoirs. This technology can be potentially implemented with an exceptionally low operating cost and also capable of producing up to 50% of the residual oil (Lazar and Constantinescu, 1997; Lazar *et al.*, 2007; Donaldson *et al.*, 2010). The field trials have shown that normal projected oil production decline curve can be reversed or leveled off by the application of MEOR and the reason is because microbial growth and metabolites produced can have effects on the chemical and physical properties of reservoir rocks and crude oil (Bryant *et al.*, 2007; Davis and Updegraff, 2009). After

the injection of these bacteria into the reservoir in in-situ application, to determine the time these bacteria have multiplied, migrated and completely soaked the entire residual oil in the reservoir, so that the well can be opened for improved production, poses serious problem in the oil industry (Kuznetsov *et al*, 2012). Furthermore, a number of other noteworthy researchers [1, 6, 9, 11, 16-19, 21, 24-27, 29 & 31] also confined their attention in this direction under different conditions.

The mathematical modeling of the behavior of bacteria used in MEOR and its activities in the reservoir has attracted interest of researchers since long back. One-dimensional models and models extending to two and three dimensions have been developed (Chang *et al.*, 1991; Updegraff, 2003; Maurya *et al*, 2013). Islam and Gianetto (1993) derived a mathematical model for describing bacterial transport, nutrient propagation and microbial growth in porous media (Nielson *et al*, 2010). They used a successive over relaxation technique to solve the governing partial differential equations. Of these they could not solve microbial transport and nutrient propagation directly because of the absence of numerical value of some constants. Therefore, they assigned values to them in order to obtain real reservoir data. All models are based on the mass balance which will be presented later as a combination of equations. This work focuses on the mathematical modeling of equations of bacterial transport, bacterial growth and nutrient propagation in the porous media.

2. Mathematical Formulation and Governing Differential Equations

Chang *et al* (1991) proposed a model for bacterial and nutrient transport in porous media as:

$$\vec{\nabla} \cdot \vec{D} \vec{\nabla} (\varphi SC) - \vec{\nabla} \cdot (\vec{U} C) - K_m \vec{\nabla} \cdot (C \text{In} C_f) + \varphi S (\mu_b - K_d) C + \frac{QC}{V} = \frac{\partial}{\partial t} (\varphi SC) + \varphi SK_c C - K_y \rho (\sigma - \sigma_{irr}) \left(\frac{\sigma}{\varphi} \right)^h \quad (2.1)$$

where D = Bacterial Diffusion Constant, S = Aqueous Phase Saturation, φ = Porosity, C = Microbial Cell Concentration, C_f = Substrate Concentration, t = time, Q = Well Flow Rate, U = Darcy Velocity, V = Bulk Volume of Cell Block, ρ = Microbial Density, σ = Volume of deposited bacteria per pore volume, μ_b = Bacteria Growth Rate, K_m = Chemotaxis coefficient, σ_{irr} = Volume of irreversibility deposited bacteria per pore volume, K_d = Decay rate of bacteria, K_c = Clogging rate of bacteria, K_y = Declogging rate of bacteria, h = Declogging parameter.

Assuming that flow and diffusion are one-dimensional, equation (2.1) may be expressed as following;

$$\frac{\partial}{\partial x} \left[D \varphi \frac{\partial (SC)}{\partial x} \right] - \frac{\partial}{\partial x} (\vec{U} C) - K_m \frac{\partial}{\partial x} \left[C \frac{\partial}{\partial x} (\text{In} C_f) \right] + \varphi S (\mu_b - K_d) C + \frac{QC}{V} = \frac{\partial}{\partial t} (\varphi SC) + \varphi SK_c C - K_y \rho (\sigma - \sigma_{irr}) \left(\frac{\sigma}{\varphi} \right)^h \quad (2.2)$$

Assuming that chemotaxis (movement of bacteria to area of high nutrients concentration) is negligible ($K_m = 0$), and that bacteria activity does not affect the porosity ($\varphi = \text{constant}$; $K_c K_y = 0$). Under these assumptions, equation (2.2) reduces to;

$$\frac{\partial}{\partial x} \left[D \varphi \frac{\partial (SC)}{\partial x} \right] - \frac{\partial}{\partial x} (\vec{U} C) + \varphi S (\mu_b - K_d) C + \frac{QC}{V} = \frac{\partial}{\partial t} (\varphi SC) \quad (2.3)$$

Assuming D to be constant and that oil and water saturation are constant, equation (2.3) yields

$$D \varphi S \frac{\partial^2 C}{\partial x^2} - \frac{\partial}{\partial x} (\vec{U} C) + \varphi S (\mu_b - K_d) C + \frac{QC}{V} = \varphi S \frac{\partial C}{\partial t} \quad (2.4)$$

Assuming \vec{U} to be constant in equation (2.4), it is fairly easy to get following equation;

$$D\varphi S \frac{\partial^2 C}{\partial x^2} - \vec{U} \frac{\partial C}{\partial x} + \varphi S(\mu_b - K_d)C + \frac{QC}{V} = \varphi S \frac{\partial C}{\partial t} \quad (2.5)$$

Substituting $\vec{U} = -\frac{k}{\mu} \frac{\partial P}{\partial x}$ into equation (2.5), we have;

$$D\varphi S \frac{\partial^2 C}{\partial x^2} + \frac{k}{\mu} \frac{\partial P}{\partial x} \cdot \frac{\partial C}{\partial x} + \varphi S(\mu_b - K_d)C + \frac{QC}{V} = \varphi S \frac{\partial C}{\partial t} \quad (2.6)$$

Assuming the term $\frac{\partial P}{\partial x} \frac{\partial C}{\partial x}$ to be very small and negligible, the equation (2.6) further yields;

$$D\varphi S \frac{\partial^2 C}{\partial x^2} + \varphi S(\mu_b - K_d)C + \frac{QC}{V} = \varphi S \frac{\partial C}{\partial t} \quad (2.7)$$

It is remarkable here that the equation (2.7) is the final equation for bacteria transport in porous media. For nutrients transport in porous media, bacteria decay rate $K_d = 0$. Equation (2.7) becomes.

$$D_f \varphi S \frac{\partial^2 C_f}{\partial x^2} + \varphi S \mu_b C_f + \frac{QC_f}{V} = \varphi S \frac{\partial C_f}{\partial t} \quad (2.8)$$

The growth of bacteria was assumed to follow the monodkinetic approach (Monod, 2000), thus, one can get;

$$\mu_b = \frac{\mu_{max} C_f}{k_s + C_f} \quad (2.9)$$

where, μ_{max} = Maximum growth rate achievable, k_s = Substrate concentration that corresponds to the growth rate, which is half of the maximum.

For bacteria transport in porous media, the final equation to be used is;

$$D\varphi S \frac{\partial^2 C}{\partial x^2} + \varphi S(\mu_b - K_d)C + \frac{QC}{V} = \varphi S \frac{\partial C}{\partial t} \quad (2.10)$$

For nutrients transport in porous media, the final equation to be used is;

$$D_f \varphi S \frac{\partial^2 C_f}{\partial x^2} + \varphi S \mu_b C_f + \frac{QC_f}{V} = \varphi S \frac{\partial C_f}{\partial t} \quad (2.11)$$

Equations (2.10) - (2.11) are the mathematical models describing the bacteria propagation, nutrient propagation and bacteria growth. The water phase consists of water, bacteria and nutrients. The reactions are nutrients consumption and bacteria multiplication. The bacteria growth rate is the Monod expression (Monod, 2000). Therefore, the reaction rate depends on the bacteria and nutrient propagation.

3. Operating Parameters

In order to solve the system of second order differential equations (2.10)-(2.11), experimental data and parameters obtained from Garzan oil field presented in Table 3.1 were used.

Table 3.1. Values for the parameters used in the mathematical model Chang *et al*(1991).

Number of grids	5
Δx , Grid length(ft)	100
D_f , Nutrient Diffusion Constant(ft ² /day)	1
D , Bacterial Diffusion constant (ft ² /day)	3
K_s , Maximum bacterial growth rate, 1/day	2

K_d , Bacterial Decay Rate 1/day	0.022
Q, Bacterial Injection Rate STB/day	200
Q_f , Nutrient Injection Rate STB/day	200
Injection Period, days	10
C, Bacterial Concentration lb/ft ³	5
C_f , Nutrient Concentration lb/ft ³	40
Δt , time steps in injection period, days	10
Duration of Shut-in Period, days	30
Δt , time step in shut-in period, days	10
Δy , Grid height, ft	50
H, height of reservoir, ft	20
Φ , Porosity	0.4
S_w , water Saturation	0.3
μ_b Bacterial growth rate, r/day	0.8

4. Solution Using Finite Difference Approximation Technique

The model equations obtained in this work were solved using finite difference approximation technique. Central difference approximation was applied in space and backward difference approximation was also applied in time at a time step (n+1) using implicit formulation. The following equation was obtained;

$$(D\varphi S)_i \frac{C_{i-1}^{n+1} - 2C_i^{n+1} + C_{i+1}^{n+1}}{(\Delta x)^2} + (\varphi S(\mu_b - K_d))_i C_i^{n+1} + \left(\frac{Q}{V}\right)_i C_i^{n+1} = (\varphi S)_i \frac{(C_i^{n+1} - C_i^n)}{\Delta t} \quad (4.1)$$

Multiplying all terms by $(\Delta x)^2$

$$(D\varphi S)_i (C_{i-1}^{n+1} - 2C_i^{n+1} + C_{i+1}^{n+1}) + [\varphi S(\Delta x)^2(\mu_b - K_d)]_i C_i^{n+1} + \left[\frac{Q(\Delta x)^2}{V}\right]_i C_i^{n+1} = [\varphi S(\Delta x)^2]_i \frac{(C_i^{n+1} - C_i^n)}{\Delta t} \quad (4.2)$$

The unknown parameters are the C-terms at the time level n+1. Collecting the unknown parameters to the left hand side and the known parameters to the right hand side of the equation, we have;

$$C_{i-1}^{n+1} - 2C_i^{n+1} + C_{i+1}^{n+1} + \left[\frac{(\Delta x)^2}{D}(\mu_b - K_d)_i\right] C_i^{n+1} + \left(\frac{Q(\Delta x)^2}{DV\varphi S}\right)_i C_i^{n+1} = \left(\frac{(\Delta x)^2}{D\Delta t}\right)_i C_i^{n+1} - \left(\frac{(\Delta x)^2}{D\Delta t}\right)_i C_i^n \quad (4.3)$$

Re-arranging equation (4.3);

$$C_{i-1}^{n+1} + \left[-2 + \frac{(\Delta x)^2}{D}(\mu_b - K_d)_i + \left(\frac{Q(\Delta x)^2}{DV\varphi S}\right)_i - \left(\frac{(\Delta x)^2}{D\Delta t}\right)_i\right] C_i^{n+1} + C_{i+1}^{n+1} = -\left(\frac{(\Delta x)^2}{D\Delta t}\right)_i C_i^n \quad (4.4)$$

For bacteria and nutrients transport, we have following equations respectively;

$$C_{i-1}^{n+1} + \left[-2 + \frac{(\Delta x)^2}{D}(\mu_b - K_d)_i + \left(\frac{Q(\Delta x)^2}{DV\varphi S}\right)_i - \left(\frac{(\Delta x)^2}{D\Delta t}\right)_i\right] C_i^{n+1} + C_{i+1}^{n+1} = -\left(\frac{(\Delta x)^2}{D\Delta t}\right)_i C_i^n \quad (4.5)$$

$$C_{f\ i-1}^{n+1} + \left[-2 - \left(\frac{(\Delta x)^2 \mu_b}{D_f}\right)_i + \left(\frac{Q(\Delta x)^2}{D_f V \varphi S}\right)_i - \left(\frac{(\Delta x)^2}{D_f \Delta t}\right)_i\right] C_{f\ i}^{n+1} + C_{f\ i+1}^{n+1} = -\left(\frac{(\Delta x)^2}{D\Delta t}\right)_i C_{f\ i}^n \quad (4.6)$$

The mathematical model equations were solved for concentrations of bacteria and nutrients in different grid blocks at different time steps. The equations were solved numerically using implicit finite difference technique where the

component mass balances and the total volume balance are satisfied. The reservoir was assumed to be a perfect rectangular shape and the volume was subdivided into volume blocks for easier testing of the effects of bacteria activity in each grid block. Each discretization point corresponds to a volume block at a specific time. It is assumed that each block is well mixed with the same composition in the entire block. The soaking period is the time it takes the bacteria, from the point of injection, to multiply and distribute and soak the entire reservoir. No flow boundary condition was assumed and the injection of bacteria and nutrients occurred throughout the first time step (10days) in the first grid block. After the first time step, the well was shut-in and the concentrations of bacteria in the other grid blocks were calculated. During the injection period, the concentrations at the inlet were calculated using the injection value. After the termination of the injection, when the well was shut-in, the injection value becomes zero. No flow boundary conditions were applied during the soaking period. This is described in Figure 4.1 where q_{sc} is the injection rate.

The equations for bacteria transport and nutrients propagation were solved to determine the concentrations of bacteria and nutrients in each grid block at different time steps, where $i = 1, 2, 3, \dots, 5$. The equations obtained were represented in matrix form for both bacteria transport and nutrients transport.

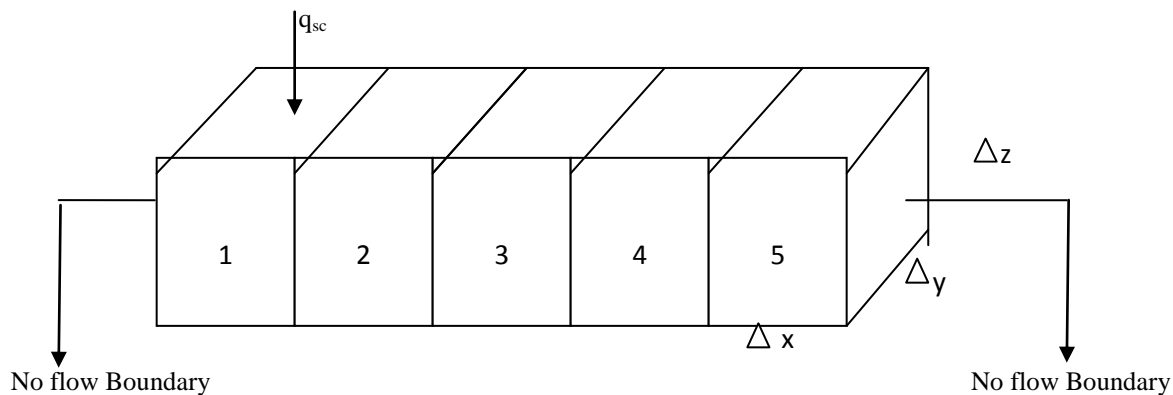


Figure 4.1. One dimensional discretization of a homogenous reservoir

5. Simulated Results

The results obtained from the model equations (2.10) and (2.11) predictions were compared with the plant data obtained from Garzan oil field as shown in Tables 5.2-5.5 for bacteria concentrations for a period of 10-40 days and Tables 5.6-5.9 for nutrient concentrations for a period of 10-40 days respectively.

Table 5.2. Bacteria, Timestep 1 (10 days)

Parameters	Model Prediction (lb/ft ³)	Garzan Oil Field Model (lb/ft ³)	Percentage deviation
C_1^{n+1}	11.1	11.6	4.3
C_2^{n+1}	12.1	11.2	8.04
C_3^{n+1}	0.17	0.2	9.8
C_4^{n+1}	0	0	0
C_5^{n+1}	0	0	0

Table 5.3. Bacteria, Timestep 2 (20 days)

Parameters	Model Prediction (lb/ft ³)	Garzan Oil Field Model (lb/ft ³)	Percentage deviation

C_1^{n+1}	26	26.4	7.6
C_2^{n+1}	16	15.2	5.26
C_3^{n+1}	5.3	6	11.6
C_4^{n+1}	0.61	0.8	9.8
C_5^{n+1}	0	0	0

Table 5.4. Bacteria, Timestep 3 (30 days)

Parameters	Model Prediction (lb/ft ³)	Garzan Oil Field Model (lb/ft ³)	Percentage deviation
C_1^{n+1}	14	15.2	7.8
C_2^{n+1}	40	39	2.6
C_3^{n+1}	40	38	5.3
C_4^{n+1}	7	7.5	6.7
C_5^{n+1}	0.14	0.1	4

Table 5.5. Bacteria, Timestep 4 (40 days)

Parameters	Model Prediction (lb/ft ³)	Garzan Oil Field Model (lb/ft ³)	Percentage deviation
C_1^{n+1}	9	10.2	11.8
C_2^{n+1}	30	28	7.1
C_3^{n+1}	20	19	5.3
C_4^{n+1}	2	2.5	11.6
C_5^{n+1}	0.5	0.9	12.6

Table 5.6. Nutrient, Timestep 1 (10 days)

Parameters	Model Prediction results (lb/ft ³)	Garzan Oil Field Model Result (lb/ft ³)	Percentage deviation
C_{f1}^{n+1}	34	32	6.25
C_{f2}^{n+1}	2	1.4	15.5
C_{f3}^{n+1}	0.18	0.2	9.8
C_{f4}^{n+1}	0	0	0
C_{f5}^{n+1}	0	0	0

Table 5.7. For Nutrient, Timestep 2 (20 days)

Parameters	Model Prediction results (lb/ft ³)	Garzan Oil Field Model Result (lb/ft ³)	Percentage deviation
C_{f1}^{n+1}	10	11	9.09
C_{f2}^{n+1}	5	6	16.7
C_{f3}^{n+1}	2	1.8	11.1

C_{f4}^{n+1}	0.2	0.3	16.7
C_{f5}^{n+1}	0	0	0

Table 5.8.Nutrient, Timestep 3 (30 days)

Parameters	Model Prediction results (lb/ft ³)	Garzan Oil Field Model Result (lb/ft ³)	Percentage deviation
C_{f1}^{n+1}	3	2.5	18.9
C_{f2}^{n+1}	5	5.3	5.7
C_{f3}^{n+1}	1.5	2	18.6
C_{f4}^{n+1}	0.2	0.18	16
C_{f5}^{n+1}	0	0	0

Table 5.9.For Nutrient, Timestep 4 (40 days)

Parameters	Model Prediction results (lb/ft ³)	Garzan Oil Field Model Result (lb/ft ³)	Percentage deviation
C_{f1}^{n+1}	0.8	0.7	14.3
C_{f2}^{n+1}	2.3	2.2	8.9
C_{f3}^{n+1}	0.3	0.5	22
C_{f4}^{n+1}	0.1	0.3	18.2
C_{f5}^{n+1}	0	0	0

6. Graphical Representation of the Simulated Results

6.1 Variation of Nutrient Concentration at the Different Grids with Time

Figure 6.1 shows that the nutrients concentration, with the combined effects of microbial consumption and diffusion, changed considerably within the reservoir.

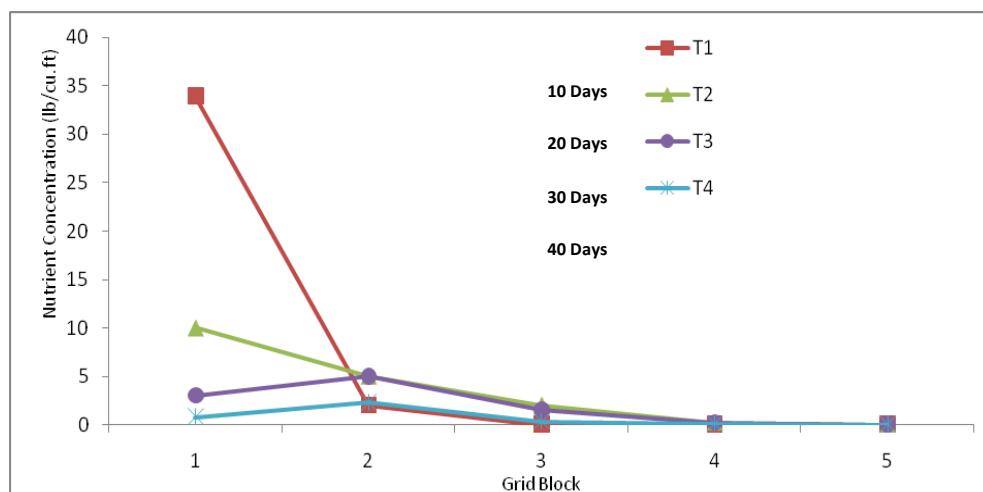


Figure 6.1. Nutrient concentration distribution at different time steps

The nutrients diffused deep into the system with each time step (10 days) and came close to the other end after time step four (40 days). The plot of T1-timestep (10days) showed how the concentration of nutrients reduced rapidly because of its consumption by bacteria. T2-timestep2 (20days) and T3-timestep3 showed how the concentration of nutrients continued to reduce sparingly as bacteria consumption increased. The Microbial consumption of the nutrients was so severe that after T4-timestep4 (40days), the available nutrients diminished completely.

6.2 Variation of Bacteria Concentration at the Different Grids with Time

It can be observed from Figure 6.2 that the bacteria concentration in the system increased as the nutrients were consumed with time. Although some of the bacteria died with time, this bacterial decay could not significantly slow down the overall increase in the bacterial population at earlier times.

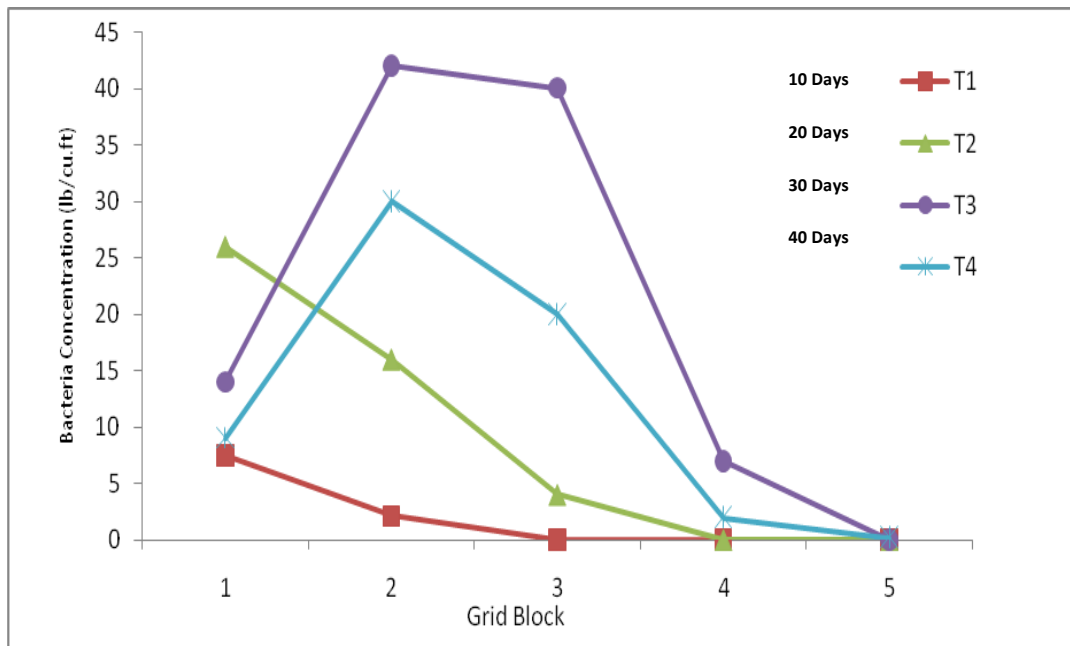


Figure 6.2. Concentration of bacteria in each grid block at different time steps

The plot of T1-timestep1 (10 days) showed how the concentration of bacteria did not change considerably because of lack of sufficient nutrients consumption. T2-timestep2 (20 days) and T3-timestep3 (30 days) showed how bacteria concentration increased significantly when nutrients consumption became more pronounced. However, after T4-timestep (40 days), lack of nutrients reversed the conditions so that the decay of micro-organisms became more severe than their multiplication. Therefore, the microbial concentration at the inlet became lower after 40days than it was during the first 20 days.

6.3 Variation of Nutrient and Bacteria Concentrations in Grid Block 1 with Time

Figure 6.3 shows how nutrients and bacteria concentrations changed in grid block 1 at different time steps. At the first time step (10 days), when there was injection of bacteria and nutrient into the reservoir, the concentration of nutrients was large while the concentration of bacteria was low.

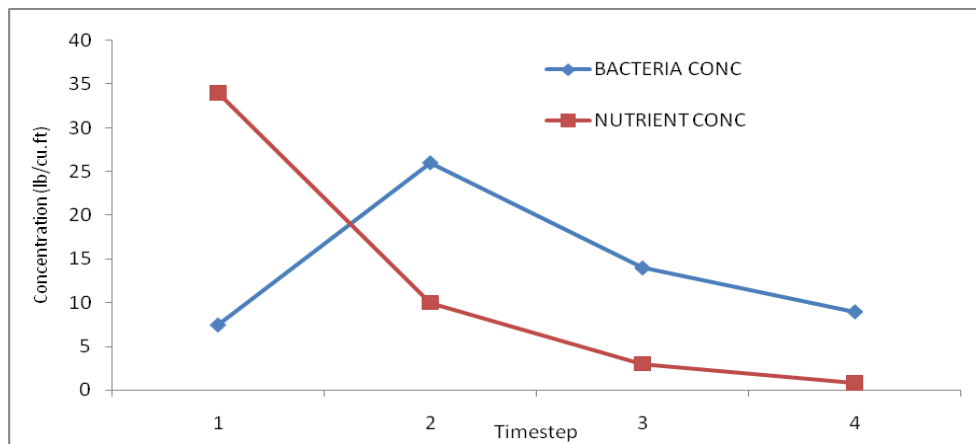


Figure 6.3. Nutrient and bacteria concentrations in grid block 1 with time

During timestep2 and timestep3, bacteria fed on the nutrients and multiplied while the nutrient concentration reduced. Timestep4 showed how the concentration of the nutrients diminished and the decay of bacteria became more pronounced, therefore, the bacteria concentration reduced as a result.

6.4 Variation of Nutrient and Bacteria Concentrations in Grid Block 2 with Time

Figure 6.4 shows that the concentration of nutrients decreased during timestep2 and timestep3 when nutrients consumption was strong, but the concentration of bacteria increased significantly indicating good nourishment and rapid growth.

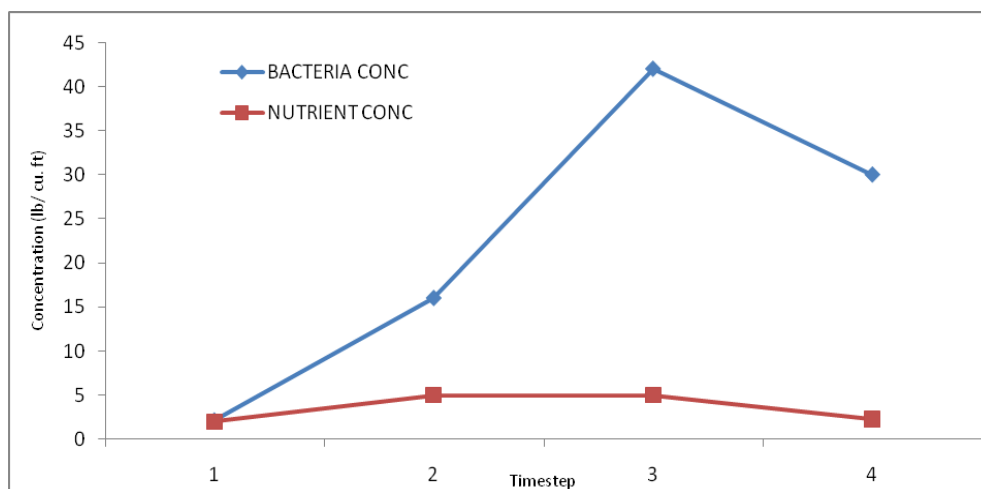


Figure 6.4. Nutrients and bacteria concentration in grid block 2 with time

As nutrients diminished during timestep4, bacteria concentration starts to drop significantly due to shortage of nutrients.

6.5 Variation of Nutrient and Bacteria Concentrations in Grid Block 3 with Time

Figure 6.5 shows how bacteria concentration increased exponentially and the nutrients concentration diminished with time. This indicates that there was good nourishment during the first three time steps. During the fourth time step, bacteria concentration began to diminish when nutrients concentration finished completely. But during the first three time steps, though the concentration of nutrients was almost finished, bacteria concentration continued to increase.

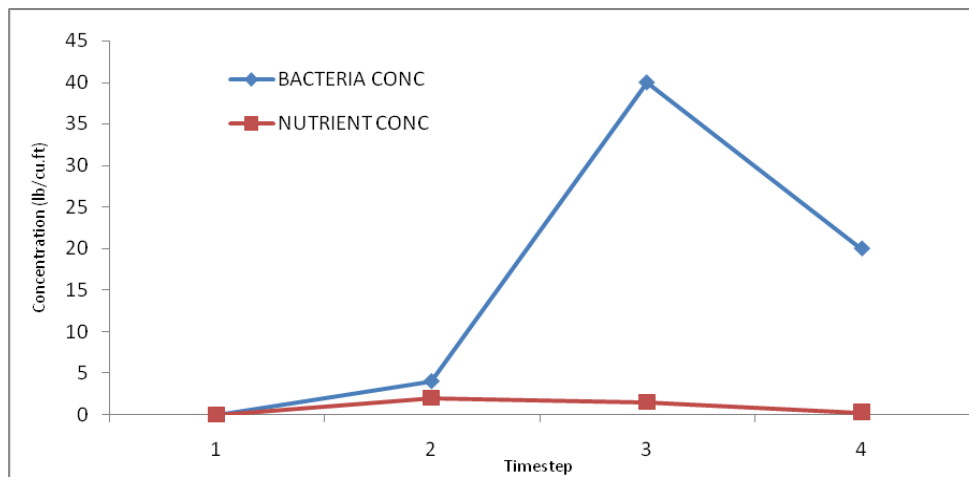


Figure 6.5. Nutrient and bacteria concentration in grid block 3 with time.

This indicates that the bacteria were not only feeding from the injected nutrients but also from the substrates present in the reservoir and its concentration continued to increase. But as the nutrients and the substrates diminished completely during the fourth time step, bacteria decay became more pronounced.

6.6 Variation of Nutrient and Bacteria Concentration in Grid Block 4 with Time

Figure 6.6 shows how the bacteria concentration increased exponentially even when nutrients concentration was low during time step 2 and time step 3, and dropped sharply as the nutrients diminished completely during time step 4.

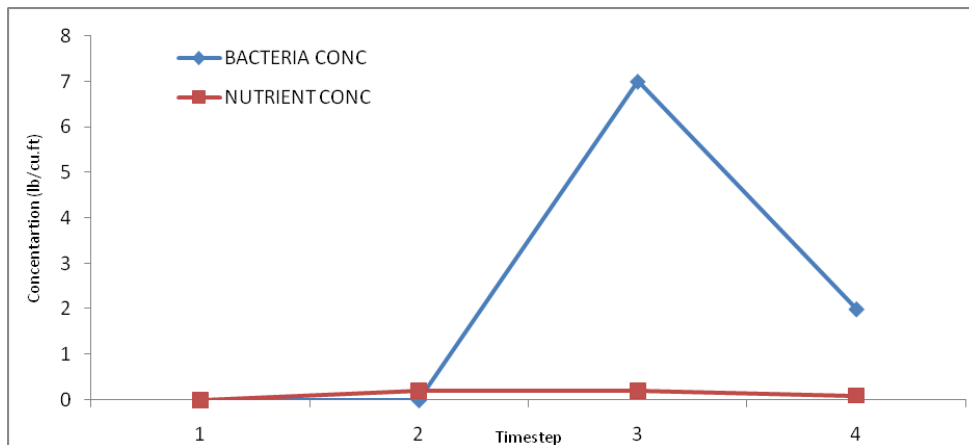


Figure 6.6. Nutrient and bacteria concentrations in grid block 4 with time

Time step 1 was the acclimatization period of the bacteria to the reservoir environment before pronounced during time step 2. The bacteria concentration continued to increase, even when nutrients concentration diminished completely, as the bacteria consumption of the substrates continued. The nutrient and the substrate concentrations simultaneously diminished completely during time step 4 and hence the decay of bacteria..

6.7 Variation of Nutrient and Bacteria Concentration in Grid Block 5 with Time

Figure 6.7 shows that time step 1 and 2 were the acclimatization period of the bacteria to the reservoir environment before the concentration of bacteria increased exponentially and dropped sharply as nutrients diminished completely. The total period it took the bacteria from the point of injection into the reservoir, to multiply and distribute and cover the whole reservoir, is called the soaking period in MEOR application. It is believed that at this point, the bacteria would

have produced enough by-products or metabolites that would not only reduce the viscosity of the oil, but also increase its mobility in the reservoir. and thereby reduce cost of production by increasing products yields.

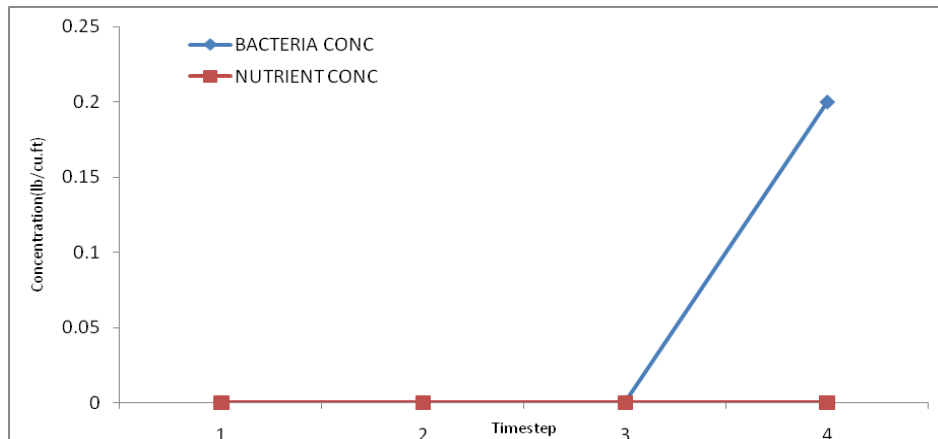


Figure 6.7. Nutrients and bacteria concentration in grid block 5 with time.

7. Conclusive Observations

Mathematical models that describe the transport of bacteria and the nutrients in the reservoir during the shut-in period have been presented here. The model parameters were obtained from a functional depleted reservoir and some unknown parameters were estimated from experimental work. The developed mathematical models were integrated numerically using the finite difference technique. The simulated results obtained from the model equations were compared with the data obtained from Garzan oil field in Turkey and it showed reasonable agreement. The results explored in the present study showed that the bacterial concentration increased as the nutrients were consumed with time. After the second timestep (20 days), due to the shortage of nutrients, the bacteria start to decay. The period the bacteria starts to decay can be taken as the period to either replenish the nutrients in a multi-step nutrient slug injection, if the bacterial concentration has not reached a certain concentration, or it could be interpreted that the bacteria has completely soaked the reservoir and it should be opened for improved oil recovery (Bryant and Lockhart, 2002).

Notations

D	Bacterial Diffusion Constant, ft ² /day
S	Aqueous Phase Saturation,
Φ	Porosity,
C	Microbial Cell Concentration, lb/ft ³
C _f	Substrate Concentration, lb/ft ³
t	time, days
Q	Well Flow Rate, STB/day
U	Darcy Velocity, ft/sec
V	Bulk Volume of Cell Block, STB
ρ	Microbial Density, lb/ft ³
σ	Volume of deposited bacteria per pore volume,
μ_b	Bacteria Growth Rate, 1/day
K _m	Chemotaxis coefficient,
σ_{irr}	Volume of irreversibility deposited bacteria per pore volume,
K _d	Decay rate of bacteria, 1/day

K_c	Clogging rate of bacteria, 1/day
K_y	Declogging rate of bacteria, 1/day
h	Declogging parameter
μ_{max}	Maximum growth rate achievable, 1/day
k_s	Substrate concentration that corresponds to the growth rate, lb/ft ³
q_{sc}	injection rate, STB/day

References

- [1] Aldoss, T.K.; Al-Nimr, M.A.; Jarrah, M.A. and Al-Shaer, B., Mixed convection flow from a vertical plate embedded in porous medium in the presence of magnetic field, *Heat Transfer*, Vol. 28(A), pp. 635-645, 1995.
- [2] Bryant R.S, Burchfield, T., Chase, K., Bertus, K., and Stepp, A., Optimization of oil mobilization, transport of microbes and metabolites, and effects of additives. In: SPE 19686 presented in 64th Annual Technical Conference and Exhibition of the Society of Petroleum Engineers held in San Antonio, TX, pp. 567-578, 1989.
- [3] Bryant, S.L., and Lockhart, T.P., Reservoir engineering analysis of microbial enhanced oil recovery, *Society of Petroleum Engineers, Reservoir Evaluation Engineering*, 5, pp. 365-374, 2002.
- [4] Chang M.M., Chung, F., Bryant, R., Gao, H., and Burchfield T., Modelling and laboratory investigation of microbial transport phenomena in porous media. In: SPE 22845 presented at 66th Annual Technical Conference and exhibition of SPE in Dallas Texas, 1991.
- [5] Davis, J.B., and Updegraff D.M , *Microbiology in the Petroleum industry*. Bacteriology Review 18, pp. 215-238, 1954.
- [6] Derek, C.; Tretheway, D.C. and Mainhart, C.D., Apparent fluid slip at hydrophobic micro channel walls, *Physics of Fluids*, Vol. 14, L9-L12, 2002.
- [7] Donaldson E.C., Chiligrarian, G.V. and Yen, T.F., Microbial enhanced oil recovery. *Developments in Petroleum Science*, 21. Amsterdam: Elsevier. pp. 227, 1989.
- [8] Islam, M. and Gianetto, A., Mathematical Modelling and Scaling Up of Microbial Enhanced Oil Recovery, *Journal of Canadian Petroleum Technology*, 32(4), pp. 30-36, 1993.
- [9] Jha, B.K., Effect of applied magnetic field on transient free convective flow in a vertical channel, *Indian Journal of Pure and Applied Mathematics*, Vol. 29(4), pp. 441-445, 1998.
- [10] Khaled, A.R.A and Vafai, K., The effect of slip condition on stokes and couette flows due to an oscillating wall, *International Journal of Nonlinear Mechanics*, Vol. 39, pp. 795-809, 2004.
- [11] Kim, Y.J., Unsteady MHD convective heat transfer past a semi-infinite vertical porous moving plate with variable suction, *International Journal of Engineering Science*, Vol. 38, pp. 833-842, 2000.
- [12] Kuznetov, S.I., Ivanov, M.V., and Lyalikova, N.N., *Introduction to Geological Microbiology (translated from Russian by P.T. Broneer and C.H. Oppenheimer)*. *Introduction to Geological Microbiology*, McGraw-Hill, New York, N.Y., pp. 252, 1962.
- [13] Lake, L., *Enhanced Oil Recovery*, Prentice Hall, Englewood Cliffs, New Jersey, 1989.
- [14] Lazar, I. and Constantinescu, P., Field trials results of MEOR. *Microbes and Oil Recovery*, 1: pp. 122-131, 1997.
- [15] Lazar, I. Petrisor, I.G., and Yen, T.F., Microbial enhanced oil recovery, *Petroleum Science and Technology*, 25(11), pp. 1353-1366, 2007.
- [16] Mahmood, A. and Ali, A., The effect of slip condition on unsteady MHD Oscillatory flow of a viscous fluid in a planer channel, *Romanian Journal of Physics*, Vol. 52, Nos. 1-2, pp. 85-91, 2007.
- [17] Makinde, O.D. and Mhone, P.Y., Heat transfer to MHD Oscillatory flow in a channel filled with porous medium, *Romanian Journal of physics*, Vol. 50(9-10), pp. 931-938, 2005.
- [18] Makinde, O.D. and Osalusi, E., MHD steady flow in a channel with slip at permeable boundaries, *Romanian Journal of Physics*, Vol. 51(3-4), pp. 319-328, 2006.
- [19] Malcinde, O.D., Laminar flow in a channel of varying width with permeable boundaries, *Romanian Journal of Physics*, Vol. 40(4-5), pp. 403, 1995.
- [20] Maurya V.N., Arora Diwinder Kaur, Maurya Avadhesh Kumar, and Gautam Ram Asrey, Numerical simulation and design parameters in solar photovoltaic water pumping systems, *American Journal of Engineering Technology*, Academic & Scientific Publishing, New York, USA, Vol.1, No. 1, pp. 1-09, 2013

- [21] Mishra, J.P.; Shit, G.C. and Rath, H.J., Flow and heat transfer of a MHD visco-elastic fluid in a channel with stretching walls, *Computers and Fluids*, Vol. 37(1), 1-11, 2008.
- [22] Monod, J., The Growth of Bacterial Cultures. *Annual Review of Microbiology*, Vol. 3, pp. 371, 2000.
- [23] Nielson, S.M., Shapiro, A.A., Michelsen, M.L., and Stenby, E.H., 1D simulation for microbial enhanced oil recovery with metabolite partitioning. *Transp. Porous Media*. 85, pp. 785-802, 2010.
- [24] Pal, D.; Veerhadraiah, R.; Shivakumar, P.N. and Rudraiah, N., Longitudinal dispersion of tracer particles in a channel bounded by porous media using slip condition, *International Journal of Mathematical science*, Vol. 7, 755-764, 1984.
- [25] Raptis, A.; Massias, C. and Tzivanidis, G., Hydromagnetic free convection flow through a porous medium between two parallel plates, *Phys. Lett.*, Vol. 90(A), pp. 288-289, 1982.
- [26] Singh, K.D. and Kumar, Suresh, Free convective fluctuating flow through a porous medium with variable permeability, *Journal of Mathematical and Physical Sciences*, Vol. 27(2), pp. 141-148, 1993.
- [27] Soltani, F. and Yilmazar, U., Slip velocity and slip layer thickness in flow of concentrated suspensions, *Journal of Applied Polymer Science*, Vol. 70, pp. 515-522, 1998.
- [28] Sparrow, E.M. and Cess, R.D., The effect of a magnetic field on a free convective heat transfer, *International Journal of Heat and Mass Transfer*, Vol. 3, pp. 267-274, 1961.
- [29] Steinruck, H., About the physical relevance of similarity solution of the boundary layer flow equation describing mixed convection flow along a vertical plate, *Fluid Dynamics Research*, Vol. 32, pp. 1-13, 2003.
- [30] Updegraff, D.M., Plugging and penetration of petroleum reservoir rock by microorganism. In: E.C. Donaldson and J.B. Clark (Eds), *Proceedings of International Conference on Microbial Enhancement of Oil Recovery*. NTIS Springfield, Va., pp. 80-85, 1983
- [31] Yu, S. and Ameen, T.A., Slip low heat transfer in rectangular micro channels, *International Journal of Heat and Mass Transfer*, Vol. 44, pp. 4225-4234, 2002.